ISBN: 978-3-95450-247-9 ISSN: 2673-5490 doi: 10.18429/JACoW-IPAC2024-MOPG71

BEAM DYNAMICS STUDY FOR A HIGH-REPETITION-RATE INFRARED TERAHERTZ FEL FACILITY

Y. M. Yang, S.X Dong, B. S. Zhang, G. Y. Feng†
University of Science and Technology of China, Hefei, China

Abstract

The paper introduces design and optimization of a high-repetition-rate infrared terahertz free-electron laser (IR-THz FEL) facility, which leverages optical resonator-based FEL technology to achieve a higher mean power output by increasing pulse frequency. Electron beam of the facility will be generated from a photocathode RF gun injector and further accelerated with a superconducting linear accelerator. Taking into account the collective effects, such as space charge, coherent synchrotron radiation (CSR), and longitudinal cavity wake field impacts, beam dynamics simulation for the injector, the accelerator, as well as the bunch compressor, has been done with codes of ASTRA and CSRTrack. With optimized microwave parameters of the linac, current profile with good symmetry has been obtained and the peak current can reach 100 A.

INTRODUCTION

To achieve the demand for a tunable, high-power-light source in the long wavelength spectrum and form a complementary structure of advantages with the Hefei Advanced Light Facility (HALF) [1, 2], a high-repetition-rate infrared terahertz free-electron laser (IR-THz FEL) project are progressing in the preliminary research stage. In this paper, after RF parameters optimization, we present beam dynamics simulation results for the injector, the bunch compressor, as well as the main linac. During the beam dynamics simulations, space charge effects, CSR effects and longitudinal cavity wake field effects have been taken into account with the codes of ASTRA [3] and CSRTrack.

LAYOUT

Schematic of the IR-THz FEL facility layout is shown in Fig. 1. The injector consists of a photo cathode RF gun, an L-band accelerating section and a third-harmonic accelerating section. Electron bunches are generated from the normal conducting 1.3 GHz RF gun and the beam energy is 5 MeV at the exit of the gun. After the gun, the electron bunches are accelerated in a superconducting 9-cell TESLA cavity with resonant frequency of 1.3 GHz: ACC1. Downstream of the ACC1 section, a third-harmonic RF system (3.9 GHz), named ACC39, will be used to linearize the longitudinal phase space distribution with RF curvature distortion and to minimize the bunch tails in the subsequent chicane. At the exit of ACC39, the electron beam energy is 20 MeV. There is a bunch compressor chicane (BC) with a C-type structure downstream of the ACC39 section. Beam energy is increased to 60 MeV after passing through the main linac with two L-band superconducting 9-cell TESLA cavities, named ACC2.

The IR-THz FEL will operate in the oscillator mode, which generates FEL radiation with wavelengths ranging from 5 μm to 1000 μm. After the ACC1 section, electron bunches are deflected with a beam distribution system and THz radiation with wavelength range from 200-1000 μm can be generated after the undulator of U1. Following the ACC2 section, the electron bunches are distributed into two distinct undulators, which generate mid-infrared and far-infrared radiation respectively.

LINEARIZING ENERGY DISTRIBUTION

To compress a bunch longitudinally, the time of flight through a specific section, such as a magnetic chicane, must be shorter for the tail of the bunch than it is for the head. The usual technique starts out by introducing a correlation between the longitudinal position of the particles in the bunch and their energy using a RF accelerating system [4]. As the electron bunch enters the compression system, it undergoes a process wherein electrons with lower momentum reach the chicane initially and follow a longer path through it.

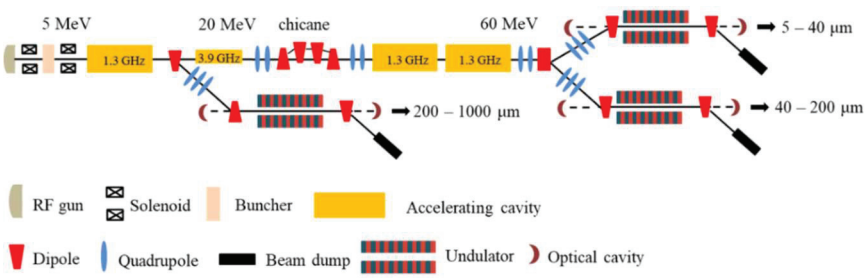

Figure 1: Schematic layout for IR-THz FEL facility.

* Work supported by Supported by the Hundred-person Program of Chinese Academy of Sciences
† fenggy@ustc.edu.cn

ISBN: 978-3-95450-247-9 ISSN: 2673-5490 doi: 10.18429/JACoW-IPAC2024-MOPG71

Conversely, those with higher momentum arrive subsequently and are directed along a shorter path within the chicane. Collectively, this dynamic results in the longitudinal compression of the electron bunch.

The non-linearities of both the accelerating RF fields and the longitudinal dispersion will distort the longitudinal phase space. The non-linearity of the fundamental RF frequency is already visible before compression as a curvature in the energy chirp. After compression, the non-linearity of the chirp, together with the T_{566} of the chicane, dominates the shape of the bunch in phase space and a sharp spike develops at the head of the charge distribution with a width depending on the intrinsic energy spread.

A higher harmonic RF system can be used to compensate the non-linearities of the fundamental frequency system and the higher order longitudinal dispersion in the magnetic chicanes. The RF phase of the harmonic section is set to the decelerating crest to compensate the 2nd-order curvature with a reasonable peak voltage. A simulation of such a compensation using a 3rd harmonic RF is shown on Fig. 2.

The sum of the accelerating voltages of the RF gun, ACC1 section and ACC39 section can be expressed by:

$$V(s) = V_g\, cos\big(\varphi_g + ks\big) + V_1\, cos(\varphi_1 + ks) + V_{39}\, cos(\varphi_{39} + 3ks)$$

where V_g and φ_g are the voltage amplitude and phase shift of the RF gun. V_i and φ_i $(i = 1, 39)$ are the voltage amplitude and phase shift of the ACC1 and ACC39. The energy distribution can be linearized if the following conditions are fulfilled:

$$\frac{dV(s)}{ds}|_{(s=0)} = const$$

$$\frac{d^2V(s)}{ds^2}|_{(s=0)} = 0, \qquad \frac{d^2V(s)}{ds^2}|_{(s=0)} = 0$$

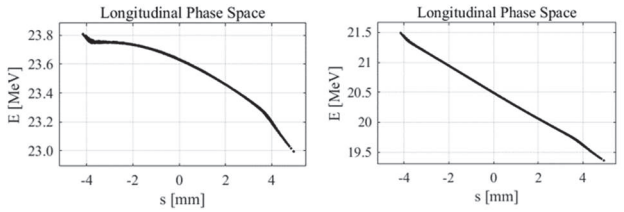

Figure 2: Longitudinal phase space before the chicane (left). The right plot shows the phase space if a 3rd harmonic RF is used to compensate the non-linearity.

BEAM DYNAMICS SIMULATION

At the entrance of the oscillator undulator section, beam bunches with high peak current, small slice emittance and low energy spread are needed to get FEL radiation with a short gain length [5, 6]. In the beam dynamics simulation, the peak current of 100 A is used and the beam energy after the main linac is 60 MeV. The beam energy before the BC section is fixed as E_1 = 20 MeV.

The transformation of the longitudinal coordinate in the i^{th} bunch compressor is described by

$$s_i = s_{i-1} - (R_{56i} \cdot \delta_i + T_{566i} \cdot \delta_i^2 + U_{5666i} \cdot \delta_i^3)$$

where R_{56i}, T_{566i} and U_{5666i} are the momentum compaction factors in the i^{th} compressor. δ_i is the relative energy deviation. For the fixed values of RF parameters and momentum compaction factors, the global compression function can be defined as follows:

$$C_N = \frac{1}{Z_N} \;,\; Z_N = \frac{\partial s_N}{\partial s}$$

where, the function $C_N(s)$ describes the increase of the peak current in the slice with initial position s and $Z_N(s)$ is the inverse global compression function. For the linear compression in the middle of the bunch, the first and the second derivatives of the global compression can be set to zero. Considering the relation between the derivative of the global compression and the derivative of the inverse global compression function, we set $Z_N' = 0$ and $Z_N'' = 0$ for the same purpose.

When excluding collective effects in a one-stage bunch compression scheme, one can establish the relationship among the RF parameters, beam energies, and inverse global compression functions.

$$E_1 = E_1(V_1, \varphi_1, V_{39}, \varphi_{39})$$

$$Z_1 = \frac{\partial^2 s_1}{\partial s^2}(0), \qquad Z_1' = \frac{\partial^2 s_1}{\partial s^2}(0), \qquad Z_1'' = \frac{\partial^3 s_1}{\partial s^3}(0)$$

The partial compression function $C_1 = 1/Z_1$ describes the amount of the compression achieved after the compressor. Z_1' can decide the symmetry of the current profile, while Z_1'' can decide the FWHM value of the bunch length [7].

As an example, consider the parameter selection for the 0.5 nC bunch charge case. Initially, the peak current after the gun is 26 A, and the compression factor is $C_1 = 4.0$. The bunch compressor chicane is operated at a bending angle of $14.5°$. Consequently, curvature radius (r) of the reference trajectory in bunch compressor chicane is set to 2.004 m. The parameter settings for the bunch compressors specific to the 0.5 nC case are detailed in Table 1.

Vectors $\overrightarrow{x_0}$ and $\overrightarrow{f_0}$ are defined as follows:

$$\overrightarrow{x_0} = \begin{pmatrix} V_1 \\ \varphi_1 \\ V_{39} \\ \varphi_{39} \end{pmatrix} \;, \qquad \overrightarrow{f_0} = \begin{pmatrix} E_1 \\ Z_1 \\ Z_1' \\ Z_1'' \end{pmatrix}$$

The relation between $\overrightarrow{x_0}$ and $\overrightarrow{f_0}$ can be written by using a nonlinear operator A_0: $\overrightarrow{f_0} = A_0(\overrightarrow{x_0})$ When the beam energies and the global compression functions are fixed, the RF parameters can be obtained by using

$$\overrightarrow{x_0} = A_0^{-1}(\overrightarrow{f_0})$$

ISBN: 978-3-95450-247-9 ISSN: 2673-5490 doi: 10.18429/JACoW-IPAC2024-MOPG71

Table 1: Parameter Settings for the Bunch Compressors

Charge Q, [nC]	r in BC, $[m]$	$R_{56,BC}, [mm]$	Compr. in BC
0.5	2.004	112.5	4.0

Table 2: RF Parameter Settings for the Accelerating Modules

Charge Q [nC]	V_{ACC1} [MV]	φ_{ACC1} [deg]	V_{ACC39}, [MV]	φ_{ACC39} [deg]	V_{ACC2} [MV]	φ_{ACC2} [deg]
0.5	18.88	9.85	3.68	145.68	40.0	19

Table 3: Beam Bunch Properties at the Entrance of the Undulator Section

Beam Energy [MeV]	Peak Current [A]	Proj. Emit. ε_x [μm]	Proj. Emit. ε_y [μm]	Slice Energy Spread σ_{max} [keV]
62.3	100	2.93	2.61	8.4

In reality, the RF parameters solution obtained above cannot produce the required compression because of the collective effects like space charge and CSR. In order to take these effects into account, a fast tracking code written in the MATLAB language is used. The RF parameter settings for the accelerating modules are shown in Table 2.

The beam dynamics simulation from the RF gun to the entrance of the undulator has been done with 100 thousand particles. For all of the arc sections, CSRTrack code is used to take into account the CSR impact. The beam tracking in the straight sections is simulated with ASTRA code. Longitudinal cavity wake field effects are considered at the exit of each accelerating section with matlab scripts.

Beam bunch properties (longitudinal phase space, current profile, slice emittances and slice energy spread) at the entrance of the undulator section are shown in Fig. 3 and Table 3. Figure 4 shows the transverse phase space (X-Y, X-X' and Y-Y') of the beam bunch. The beam quality can reach the requirements for future FEL applications.

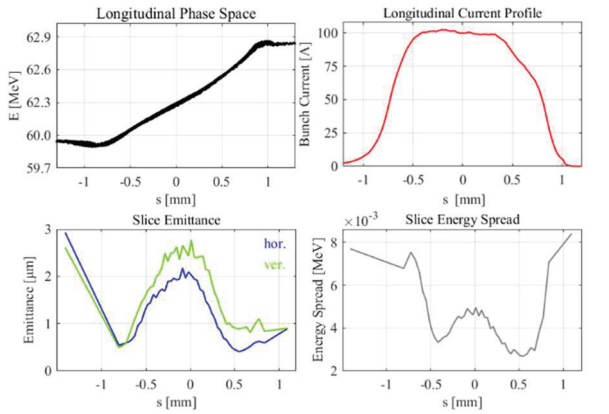

Figure 3: Longitudinal phase space (top left), current profile (top right), slice emittances (bottom left), and slice energy spread (bottom right).

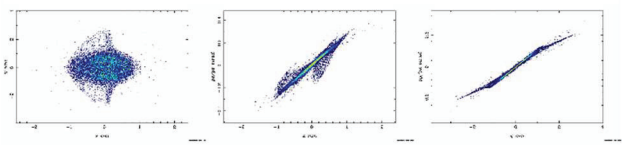

Figure 4: Transverse phase space X-Y (left), X-X' (center), and Y-Y' (right).

CONCLUSION

In the paper, the beam dynamics simulation for the high-repetition-rate IR-THz FEL facility is introduced which includes the parameters selection for the bunch compressors, the RF parameters calculation for the accelerating modules and the beam dynamics simulation taking into account the collective effects. With optimized microwave parameters of the linac, current profile with good symmetry has been obtained and the peak current can reach 100 A. The beam quality can reach the requirements for future FEL applications.

REFERENCES

[1] Z. H. Bai, G. W. Liu, T. L. He, *et al.*, "Preliminary physics design of the Hefei Advanced Light Facility storage ring", *High Power Laser and Particle Beams*, vol. 34, no. 10, pp. 104003-1–104003-6, Oct. 2022. doi:10.11884/HPLPB202234.220137

[2] K. Zhou, P. Ling, *et al.*, "General Design of Infrared Terahertz Free-Electron Laser Facility of Chinese Academy of Engineering Physics," Chin. J. Lasers, vol. 50, no. 17, pp. 1718001-1, Sep. 2023. doi:10.3788/CJL230786

[3] K. Floettmann, "ASTRA", DESY, Hamburg, https://www.desy.de/~mpyflo/

[4] W. Chou, "ICFA Beam Dynamics Newsletter", no. 38, Dec. 2005. https://icfa-usa.jlab.org/archive/newsletter/icfa_bd_nl_38.pdf

[5] G. Y. Feng, I. Zagorodnov, T. Limberg, *et al.*, " Beam Dynamics Simulation for FLASH2 HGHG Option ", in *Proc. LINAC'14*, Geneva, Switzerland, Aug.-Sep. 2014, paper TUPP020, pp. 471-474.

[6] G. Y. Feng, I. Zagorodnov, M. Dohlus, *et al.*, "Start-to-end simulation for FLASH2 HGHG Option", in *Proc. FEL'14*, Basel, Switzerland, Aug. 2014, paper MOP083, pp. 244-247.

[7] G. Y. Feng, I. Zagorodnov, T. Limberg, et al., "Beam Dynamics Simulations for European XFEL", DESY, Hamburg, TESLA-FEL2013-04 https://flash.desy.de/sites2009/site_vuvfel/content/e403/e1642/e164854/e164855/infoboxContent167617/TESLA-FEL2013-04.pdf